


# ASIC3 inhibition modulates inflammation-induced changes in the activity and sensitivity of A $\delta$ and C fiber sensory neurons that innervate bone

Molecular Pain  
Volume 16: 1–14  
© The Author(s) 2020  
Article reuse guidelines:  
sagepub.com/journals-permissions  
DOI: 10.1177/1744806920975950  
journals.sagepub.com/home/mpx  


Michael Morgan<sup>1</sup> , Jenny Thai<sup>1</sup> , Phu Trinh<sup>1</sup> ,  
Mohamed Habib<sup>1</sup>, Kelly N Effendi<sup>1</sup>  and Jason J Ivanusic<sup>1</sup> 

## Abstract

The Acid Sensing Ion Channel 3 (ASIC3) is a non-selective cation channel that is activated by acidification, and is known to have a role in regulating inflammatory pain. It has pro-algesic roles in a range of conditions that present with bone pain, but the mechanism for this has not yet been demonstrated. We aimed to determine if ASIC3 is expressed in A $\delta$  and/or C fiber bone afferent neurons, and to explore its role in the activation and sensitization of bone afferent neurons after acute inflammation. A combination of retrograde tracing and immunohistochemistry was used to determine expression of ASIC3 in the soma of bone afferent neurons. A novel, *in vivo*, electrophysiological bone-nerve preparation was used to make recordings of the activity and sensitivity of bone afferent neurons in the presence of carrageenan-induced inflammation, with and without the selective ASIC3 inhibitor APET $\times$ 2. A substantial proportion of bone afferent neurons express ASIC3, including unmyelinated (neurofilament poor) and small diameter myelinated (neurofilament rich) neurons that are likely to be C and A $\delta$  nerve fibers respectively. Electrophysiological recordings revealed that application of APET $\times$ 2 to the marrow cavity inhibited carrageenan-induced spontaneous activity of C and A $\delta$  fiber bone afferent neurons. APET $\times$ 2 also inhibited carrageenan-induced sensitization of A $\delta$  and C fiber bone afferent neurons to mechanical stimulation, but had no effect on the sensitivity of bone afferent neurons in the absence of inflammation. This evidence supports a role for ASIC3 in the pathogenesis of pain associated with inflammation of the bone.

## Keywords

Acid sensing ion channels, ASIC3, bone, pain, electrophysiology, inflammatory pain

Date Received: 9 September 2020; Revised 13 October 2020; accepted: 29 October 2020

## Introduction

Inflammation is a major component of many bony pathologies, including bone cancer, osteoarthritis and osteoporosis.<sup>1–3</sup> Cell damage or lysis following inflammation is accompanied by the production and release of extracellular protons.<sup>4,5</sup> Osteoclast-mediated bone remodeling also releases extracellular protons and is a hallmark of osteoporosis,<sup>6,7</sup> and also occurs in some types of bone cancer.<sup>7–10</sup> Extracellular protons are potent activators of peripheral sensory neurons and are therefore a likely trigger for pain in these conditions.<sup>4,11–13</sup>

Acid-sensing ion channels (ASICs) are voltage-independent proton-gated sodium channels that are activated by a drop in extracellular pH.<sup>14</sup> ASICs 1–3 are

expressed in peripheral sensory neurons where they assemble as homomeric or heteromeric channels containing three ASIC subunits to sense changes in extracellular pH.<sup>15</sup> The ASIC3 subunit is known to play a role in regulating inflammatory pain.<sup>4,16–19</sup> Furthermore, inhibiting ASIC3 attenuates pain behaviors in animal models of osteoporosis, bone cancer and

<sup>1</sup>Department of Anatomy and Neuroscience, University of Melbourne, Melbourne, Victoria, Australia

### Corresponding Author:

Jason J Ivanusic, Department of Anatomy and Neuroscience, University of Melbourne, Melbourne, VIC 3010, Australia.

Email: j.ivanusic@unimelb.edu.au



osteoarthritis,<sup>6,20–22</sup> suggesting that pharmacological manipulation of ASIC3 might provide benefit for pain management in bony pathology. ASIC3 is also upregulated in dorsal root ganglia (DRG) neurons in animal models of these same diseases,<sup>6,7,20–23</sup> further suggesting that at least some of the effects of inhibiting ASIC3 are likely due to their expression in peripheral sensory neurons that innervate bone.

Recently, toxins targeting ASICs have been isolated from a variety of venomous animals, and have been used to establish the role of ASICs in pain.<sup>24,25</sup> APET×2 is a toxin isolated from a sea anemone that selectively and effectively inhibits homomeric and heteromeric channels containing ASIC3, but does not inhibit channels formed from closely related ASIC subunits, including ASIC1 and ASIC2.<sup>26,27</sup> APET×2 has been utilized to demonstrate a role of ASIC3 containing channels in acid-induced, inflammatory and post-operative pain in rodents.<sup>16,18</sup> Inhibiting ASIC3 with APET×2 also improves pain-like behavior in a mouse model of osteoporosis<sup>6</sup> and multiple myeloma.<sup>20</sup> Whilst the specific inhibition of ASIC3 by APET×2 poses an opportunity for the treatment of pain accompanying an acidic microenvironment in bone, it is not yet clear if and how inhibiting ASIC3 with APET×2 affects the function of the sensory neurons that innervate bone (bone afferent neurons).

We have recently developed a model of acute inflammatory bone pain induced by injection of carrageenan directly into the marrow cavity of the rat tibia.<sup>28</sup> We have made electrophysiological recordings using this model to show that the activity and sensitivity of bone afferent neurons are rapidly altered by acute inflammation. The aim of the present study was to explore if and how inhibition of ASIC3 with APET×2 affects the function of different sub-populations of bone afferent neurons in this model of acute experimental inflammation in bone.

## Materials and methods

Male Sprague-Dawley rats weighing between 200 and 250 g were used in this study. Animals were housed in pairs in a 12 h light/dark cycle and were provided with food and water *ad libitum*. All experiments conformed to the Australian National Health and Medical Research Council code of practice for the use of animals in research and were approved by the University of Melbourne Animal Experimentation Ethics Committee.

### *Electrophysiological recordings using an in vivo bone-nerve preparation*

**Recording configuration.** Recordings of the activity and sensitivity of bone afferent neurons were made using an *in vivo* bone-nerve electrophysiological preparation,

described in detail in our previous publications.<sup>29–31</sup> In brief, urethane anesthetized rats (50% w/v, 1.5 g/kg i.p.) were prepared for recording. A fine branch of nerve that innervates the marrow cavity of the tibia was isolated and placed over a platinum hook electrode for extracellular recording. Whole-nerve electrical activity was amplified (1000×) and filtered (high pass 100 Hz, low pass 3 kHz) (DP-311 differential amplifier, Warner Instruments), sampled at 20 kHz (PowerLab, ADInstruments, Australia) and stored to PC using LabChart recording software (ADInstruments). A ramp-and-hold mechanical stimulus was delivered to the endings of bone afferent neurons by raising intraosseous pressure with an injection of heparinised physiological saline (0.9% sodium chloride), delivered through a needle implanted into the marrow cavity with an initial flow rate of 7 ml/min during the ramp phase, and a constant 300 mmHg of pressure delivered for 20-sec duration during the hold phase. Carrageenan (10 µl; 3% in saline; Sigma-Aldrich), APET×2 (10 µl; 1 µM in saline; Alomone) and/or saline (vehicle control) were delivered as a single injection to the marrow cavity through a second needle. The volume of the bone marrow cavity is approximately 100–200 µl, thus a 10 µl APET×2 injection will be diluted at least 10-fold. We therefore predict the local concentration of APET×2 in the marrow cavity to be approximately 0.05–0.1 µM. At this concentration, APET×2 has been shown to inhibit ASIC3 homomers (IC<sub>50</sub> of 63 nM) and heteromers (IC<sub>50</sub> of 100–2000 nM), but not Nav1.8 (IC<sub>50</sub> of 2.6 µM).<sup>26,32,33</sup> There were no changes in the pressure recorded in the marrow cavity while these agents were being injected. In a separate experiment, either saline (10 µl) or APET×2 (10 µl; 1 µM in saline) were injected into the tibia without carrageenan to determine whether inhibition of ASIC3 alone had any effect on the mechanical sensitivity of bone afferent neurons.

All action potentials (spikes) with positive and/or negative peaks clearly above noise were sampled from the whole-nerve recordings. We were unable to routinely record conduction velocities in each experiment because we could not electrically stimulate the receptive fields of individual bone afferent neurons buried deep inside the marrow cavity. Instead, we classified spikes as originating from C, Aδ or Aβ units on the basis of previously published experiments, using the same recording configuration, in which we demonstrated a linear relationship between conduction velocity and peak-to-peak action potential amplitude for units activated with mechanical stimulation from within the bone marrow.<sup>29,31</sup> On the basis of this relationship, impulses with amplitudes <40 µV were defined as originating from C fibers (conduction velocities <2.5 m/s) and those with amplitudes between 40 and 145 µV were defined as originating from Aδ fibers (conduction

velocities between 2.5 and 12.5 m/sec). For a thorough discussion of how this division was selected, see Nencini et al.<sup>29</sup> Further analyses were performed on data derived from spikes with amplitudes consistent with either A $\delta$  or C fiber conduction velocities.

**Protocols and analysis.** In a previous study, we have shown that the activity and sensitivity of bone afferent neurons are rapidly altered by acute carrageenan-induced inflammation of bone.<sup>28</sup> In particular, injection of carrageenan induced an increase in ongoing activity of bone afferent neurons, reduced their threshold for mechanical activation, and increased their discharge frequency in response to mechanical stimulation, relative to injection of saline alone. To determine if inhibition of ASIC3 could attenuate carrageenan-induced changes in the function of bone afferent neurons in the present study, we compared the activity and sensitivity of bone afferent neurons in animals injected with carrageenan and APET $\times$ 2, to that in animals injected with carrageenan and saline, and in some cases in animals injected with saline alone.

For analysis of ongoing activity, a continuous whole-nerve recording was made from 5 minutes before, to 60 minutes after injection of carrageenan and APET $\times$ 2/saline. The number of spikes before and after the injection was reported in a frequency histogram generated using 20 sec bin widths. The onset of carrageenan-induced activity was defined as the time at which the mean frequency of discharge in two consecutive 20 sec bins exceeded that of the mean frequency of discharge in all pre-injection bins. Area under the curve (AUC<sub>0-60</sub>) was determined using the trapezoid rule (spikes  $\times$  min) in GraphPad Prism (GraphPad Software).

For analysis of sensitivity to mechanical stimulation, single mechanically-activated A $\delta$ -bone marrow nociceptors were isolated from whole-nerve recordings made during application of the ramp-and-hold intra-osseous pressure stimulus using a spike discrimination software (LabChart v8.1.7, ADInstruments). Single unit discharge frequency and thresholds for mechanical activation during the pressure stimulus were determined before (baseline) and at 15 mins after application of carrageenan and APET $\times$ 2/saline. Both discharge frequency and threshold for activation were expressed as a percentage of pre-injection baseline values. Discharge frequency was reported over the entire 20 sec ramp-and-hold pressure stimulus (total response). Units with decreases in mechanical threshold greater than 20% compared to baseline threshold were defined as sensitized. We were not able to isolate individual C fiber units using our recording configuration and so cannot comment on whether single C fiber units were sensitized to mechanical stimulation. However, we report data for all spikes with amplitudes consistent with C fiber activity in whole-nerve recordings. This allows us to consider if there are

changes in the discharge frequency of C fiber units at the whole nerve level.

### Statistical analysis

Statistical analyses were performed using GraphPad Prism (GraphPad Software). For analyses of whole-nerve A $\delta$  and C fiber ongoing activity, comparisons of the area under the curve (AUC<sub>0-60</sub>) were made between treatment groups using a Student's t-test (carrageenan+APET $\times$ 2 vs carrageenan+saline). For analyses of the response of single A $\delta$  bone afferent neurons to mechanical stimulation, comparisons between treatment groups were evaluated using a mixed model nested one-way ANOVA (saline alone, carrageenan and saline, carrageenan and APET $\times$ 2) followed by Dunnett's *post hoc* analysis, or a nested t-test (saline alone, APET $\times$ 2 alone). A mixed model design was used to avoid potential errors related to pseudo replication for electrophysiological data that included multiple cells derived from a single recording preparation. For analyses of the response of C fiber activity in whole-nerve recordings, comparisons between treatment groups were made with a Kruskal-Wallis test followed by Dunn's *post hoc* analysis (saline alone, carrageenan and saline, carrageenan and APET $\times$ 2), or a Mann-Whitney test (saline alone, APET $\times$ 2 alone). *Post hoc* testing was not performed unless the ANOVA F value was significant. In all cases,  $P < 0.05$  was used to define statistical significance. In cases where multiple cells were isolated from a single recording,  $n$  = number of cells and  $N$  = number of recordings.

### Retrograde tracing and immunohistochemistry

Animals were anesthetized with isoflurane (4% induction; 2.5% maintenance). A skin incision was made over the medial aspect of the left tibia and a small hole was made in the cortical bone on the medial aspect of the tibial diaphysis using a sterile 26-gauge needle. A Hamilton syringe was used to inject the retrograde tracer Fast Blue (2  $\mu$ l FB; 10% dH<sub>2</sub>O, Illing Plastics GmbH) through the hole and directly into the medullary cavity. The hole was sealed with bone wax to prevent leakage into surrounding tissues, and the entire area was washed extensively with 0.1 M phosphate-buffered saline (pH7.4, PBS). There was no leakage to surrounding tissues. The skin incision was closed with stainless steel autoclips. Animals were left for a 10-day recovery period to allow for transport of the tracer from the medullary cavity to neuronal cell bodies located in the DRG (Figure 1(a)).

Ten-days post-surgery, animals were anaesthetized with an overdose of ketamine/xylazine (ketamine 130 mg/kg, xylazine 10 mg/kg; i.p.), and perfused via

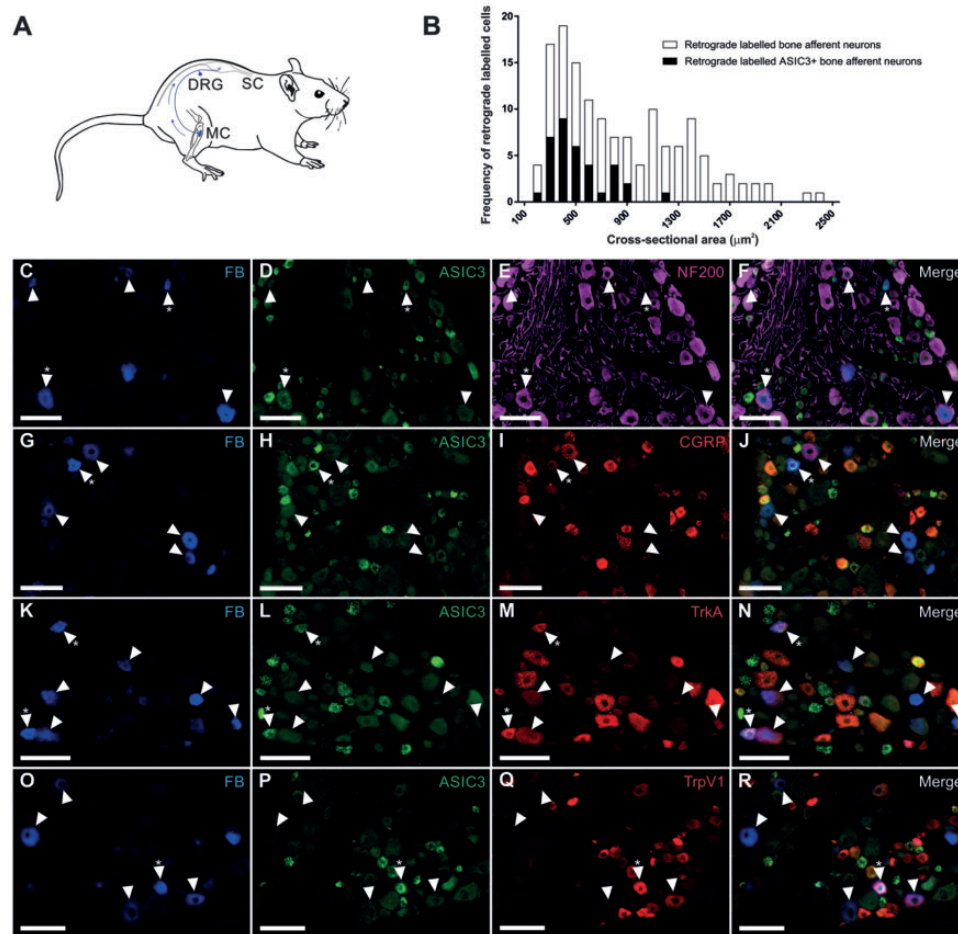


**Figure 1.** Images of retrograde labeled (Fast blue; FB) and immuno-labeled bone afferent neurons in sections through the DRG. (A) Schematic representation of the retrograde tracing approach used in this study. Fast Blue (FB) was injected into the marrow cavity (MC) of the rat tibia ( $N = 4$ ). The tracer was taken up by nerve terminals and transported back to their soma in the dorsal root ganglion (DRG), permitting identification of sensory neurons that innervate the rat tibia. (B) Size/frequency distribution of all retrograde labeled bone afferent neurons analyzed in this study. Retrograde labeled bone afferent neurons that expressed ASIC3 were mostly small or medium sized neurons ( $< 1800 \mu\text{m}^2$ ). (C)–(R) Images of retrograde and immuno-labeled bone afferent neurons in sections through the DRG. Each horizontal set of panels shows the same field of a single section. Arrowheads identify retrograde labeled bone afferent neurons throughout. Asterisks (\*) indicate bone afferent neurons that are ASIC3+. C–F shows FB (C), ASIC3 immuno-labeling (D), NF200 immuno-labeling (E) and a merged image (F). G–J shows FB (G), ASIC3 immuno-labeling (H), CGRP immuno-labeling (I) and a merged image (J). K–N shows FB (K), ASIC3 immuno-labeling (L), TrkA immuno-labeling (M) and a merged image (N). O–R shows FB (O), ASIC3 immuno-labeling (P), TrpV1 immuno-labeling (Q) and a merged image (R). Scale bars =  $100 \mu\text{m}$ .

the ascending aorta with 500 ml heparinized PBS followed by 500 ml Zamboni's fixative (2% formalin and 15% saturated picric acid in 0.1 M phosphate buffer). Lumbar DRG L3 were dissected and left overnight in 30% sucrose-PBS, then frozen in liquid nitrogen-cooled isopentane and sectioned at  $12 \mu\text{m}$  using a cryostat. Multiple series of sections were collected on gelatinized glass slides (0.1% chrome alum and 0.5% gelatin) and air-dried for one hour. Retrograde labeled cells in each section were imaged with a 10x objective, using a Zeiss Axioskop fluorescence microscope (Zeiss, Oberkochen, Germany) fitted with an AxioCam MRm camera. A DAPI UV filter was used to identify FB. Sections were

then immuno-labeled to determine if retrograde-labeled neurons expressed ASIC3, NF200 (myelinated neurons), TrkA (NGF-sensitive neurons), CGRP (peptidergic nociceptors), and/or TRPV1 (polymodal nociceptors). Details of the primary and secondary antibodies are provided in Table 1. All antibodies were diluted in PBS containing 0.3% Triton X-100 and 0.1% sodium azide. Sections were washed three times in PBS and blocked for one hour in PBS containing 10% normal horse serum and 1% Triton X-100, and then incubated overnight in the primary antisera at room temperature. In cases where double or triple labeling was used to identify colocalization of ASIC3 and NF200 with TrkA,

**Table 1.** Details of the primary and secondary antibodies in this study.

Primary antibody	Immunogen	Manufacturing details	Specificity/ characterization	Dilution
Acid sensing ion-channel 3 (ASIC3)	Corresponding to residues 285-304 of the extracellular domain rat ASIC3	Neuromics; guinea pig polyclonal; #GP14105	41-43	1:300
Calcitonin gene-related peptide (CGRP)	Synthetic rat CGRP conjugated to KLH	Sigma-Aldrich; rabbit polyclonal; #C8198	34,35	1:1000
Neurofilament 200 (NF200)	Carboxyterminal tail segment of pigneurofilament H-subunit	Sigma-Aldrich; mouse monoclonal; #N0142	36	1:1000
Tyrosine receptor kinase A (TrkA)	Purified recombinant rat TrkA extracellular domain (Ala33-Pro418)	R&D Systems; goat polyclonal; #AF1056	37	1:1000
Transient receptor potential Vanilloid 1 (TRPV1)	Intracellular C-terminus of rat TRPV1 (824-838)	Alomone Labs; rabbit polyclonal; #ACC-030	38,39	1:1000
Secondary antibody	Manufacturing details			Dilution
Donkey anti-Goat Alexa Fluor 594	Jackson Immuno- Research, #705-585-147			1:200
Donkey anti-Guinea Pig Alexa Fluor 488	Jackson Immuno- Research, #706-545-148			1:200
Donkey anti-Mouse Alexa Fluor 647	Molecular probes, Invitrogen, #A31571			1:200

CGRP or TRPV1, all antibodies were diluted in the same incubation solution. The following day, sections were washed three times and incubated in secondary antibody for 2 hours at room temperature. Following another three washes, the slides were cover-slipped using DAKO (Carpentaria, CA) fluorescence mounting medium.

Immuno-labeling of DRG sections was examined and photographed with a 10x objective using a Zeiss Axioskop fluorescence microscope (Zeiss, Oberkochen, Germany) fitted with an AxioCam MRm camera. FITC, Texas Red and Cy5 filter sets were used to discriminate labeling with the Alexa Fluor 488, 594 and 647 fluorophores, respectively. Images of immuno-labeled cells were aligned with those taken of retrograde labeled cells by using landmarks such as the edge of the section, surrounding blood vessels and other cells. Cell counts and soma size measurements (cross-sectional area of soma;  $\mu\text{m}^2$ ) were made directly from images using Zen Lite software (Zen 2011, Zeiss, Oberkochen, Germany). Cells were classified on the basis of soma size as small ( $<800 \mu\text{m}^2$ ), medium ( $800\text{--}1800 \mu\text{m}^2$ ), or large ( $>1800 \mu\text{m}^2$ ).<sup>40</sup> To prevent double counting, sections on each series were taken  $60 \mu\text{m}$  apart and only cells with a nucleus visible under the microscope were examined. We determined the proportion of retrograde labeled bone afferent neurons that expressed each antibody marker for each animal and presented it as mean  $\pm$  SEM (%). Figures were prepared using CorelDraw software (CorelDraw Graphics Suite, Ottawa, Canada).

Individual images were contrast and brightness adjusted. No other manipulations were made to the images.

### Antibody specificity

The ASIC3 antibody (polyclonal guinea pig anti-ASIC3, Neuromics, #GP14105) is raised against the extracellular domain of rat ASIC3 (corresponding to amino acid residues 285–304). The specificity of the antibody has been validated in the nodose ganglia of ASIC3 knockout mice, which show no ASIC3 immunoreactivity.<sup>41</sup> It labels ASIC3-transfected COS-7 cells, but not cells transfected with ASIC1a, 1b or 2.<sup>42</sup> Preabsorption with rat ASIC3 abolishes immuno-labeling in rat trigeminal ganglia<sup>43</sup> and DRG.<sup>42</sup> It does not label tissue in the brainstem, which has no reported ASIC3 mRNA,<sup>42</sup> and omission of the primary antibody resulted in no labelling in rat DRG<sup>42</sup> and in the current study. Indistinguishable results were obtained when the antibody was compared with another ASIC3 antibody, raised in a different host species, to label vascular innervation.<sup>42</sup> The CGRP antibody (polyclonal rabbit anti-CGRP, Sigma-Aldrich, #C8198) is raised in rabbit against synthetic rat CGRP conjugated to keyhole limpet hemocyanin. This antibody binds to rat and human CGRP, and human  $\beta$ -CGRP, but has no cross-reactivity with other peptides (manufacturer's information). Immuno-staining of sensory nerve terminals in rat glabrous skin,<sup>34</sup> and the rat spinal dorsal horn,<sup>35</sup> was abolished when the antibody was preabsorbed with rat CGRP. The NF200 antibody

**Table 2.** The percentage of retrograde labeled bone afferent neurons that express ASIC3, TrkA, TRPV1, NF200 and CGRP in the DRG.

	Number of animals	Number of retrograde labeled bone afferent neurons	Percentage (mean $\pm$ SEM)
Percentage of bone afferent neurons that are:			
ASIC3+	4	171	29 $\pm$ 3
TrkA+	4	171	61 $\pm$ 5
TRPV1+	4	142	30 $\pm$ 5
CGRP+	4	144	43 $\pm$ 8
Proportion of myelinated (NF200+) bone afferent neurons that expressed ASIC3	4	171	13 $\pm$ 4
Proportion of unmyelinated (NF200-) bone afferent neurons that expressed ASIC3	4	171	61 $\pm$ 5
Proportion of ASIC3 bone afferent neurons that are myelinated (NF200+)	4	171	26 $\pm$ 7
Proportion of ASIC3 bone afferent neurons that are unmyelinated (NF200-)	4	171	74 $\pm$ 7
Proportion of ASIC3 bone afferent neurons that express CGRP	4	144	74 $\pm$ 9
Proportion of ASIC3 bone afferent neurons that express TrkA	4	171	72 $\pm$ 11
Proportion of ASIC3 bone afferent neurons that express TRPV1	4	142	49 $\pm$ 9

(monoclonal mouse anti-NF200, clone N52, Sigma-Aldrich, #N0142) is raised against the carboxy-terminal tail segment of porcine neurofilament H-subunit. Western blot analysis of the rat DRG using this antibody showed a single band at 200-kDa, and preincubation with porcine NF200 abolished immunostaining in DRG sections.<sup>36</sup> The TrkA antibody (polyclonal goat anti-TrkA, R&D Systems, #AF1056) is raised against the extracellular domain of rat TrkA (Ala33-Pro418), and showed less than 1% cross-reactivity with recombinant mouse TrkB and TrkC in direct ELISA and Western blot (manufacturer's information). Staining of rat trigeminal ganglia was abolished when this antibody was preabsorbed with a blocking peptide.<sup>37</sup> The TRPV1 antibody (polyclonal rabbit anti-TRPV1, Alomone, #ACC-030,) is raised against the intracellular c-terminus of rat TRPV1 (corresponding to amino acids 824–838). Immuno-staining using this antibody was absent in the trigeminal ganglia of TRPV1 knockout mice but was present in wild-type controls.<sup>38</sup> Staining was also abolished in guinea pig corneal epithelium and rat DRG when it was preabsorbed with TRPV1 control peptide.<sup>39</sup>

## Results

### *ASIC3 is expressed in medium diameter myelinated (A $\delta$ fiber) and small diameter unmyelinated (C fiber) bone afferent neurons*

We used a combination of retrograde tracing and immunohistochemistry to determine the proportion of bone afferent neurons that express ASIC3, and/or other pain

signaling molecules (TrkA, TRPV1 and CGRP) (Figure 1). Retrograde labeled bone afferent neurons were predominantly small or medium sized neurons (>93% of those counted were less than 1800  $\mu\text{m}^2$ ). ASIC3 was expressed in approximately one third of bone afferent neurons (29  $\pm$  3%; Table 2). The majority of ASIC3 expressing bone afferent neurons were unmyelinated (NF200-; 74  $\pm$  7%; Table 2), but some were myelinated (NF200+; 26  $\pm$  7%; Table 2). Most ASIC3 expressing bone afferent neurons expressed CGRP (74  $\pm$  9%; Table 2) or TrkA (72  $\pm$  11%; Table 2), and half expressed TRPV1 (49  $\pm$  9%; Table 2). Interestingly, more than half of all unmyelinated (NF200-) bone afferent neurons expressed ASIC3 (61  $\pm$  5%; Table 2). A much smaller proportion of myelinated (NF200+) bone afferent neurons expressed ASIC3 (13  $\pm$  4%; Table 2). These findings show that ASIC3 is expressed in both A $\delta$  and C bone afferent neurons, and suggest that most ASIC3 expressing bone afferent neurons are NGF-sensitive, peptidergic nociceptors.

### *Inhibition of ASIC3 decreases carrageenan-induced activity of A and C fiber bone afferent neurons*

To determine whether ASIC3 contributes to acute inflammation-induced increases in the activity of bone afferent neurons, ongoing activity was assayed in animals treated with carrageenan+APET $\times$ 2 (Figure 2(b)), and was compared to activity assayed in animals treated with carrageenan+saline (Figure 2(a)). There was a rapid, carrageenan-induced increase in the activity of A $\delta$  bone afferent neurons recorded from animals co-injected with saline (latency to onset of 3.5  $\pm$  1.3 min), that subsided within 30 minutes (Figure 2(c)). In

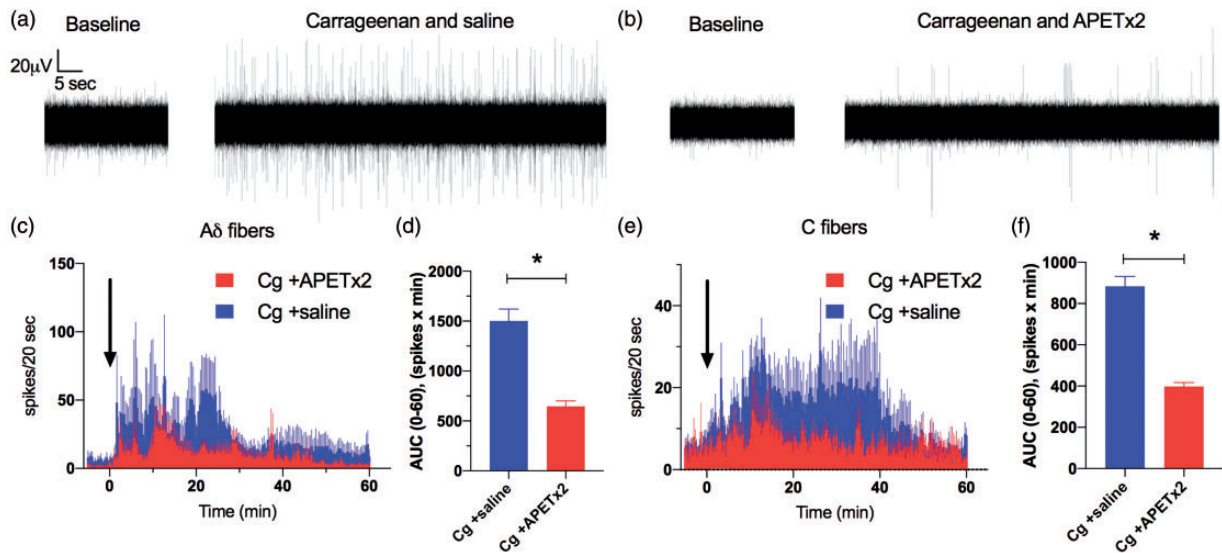


**Figure 2.** Inhibition of ASIC3 with APETx2 inhibits carrageenan-induced activity in A $\delta$  and C fiber bone afferent neurons. (a) and (b) are examples of whole-nerve recordings before (baseline) and after application of carrageenan+saline (a) or carrageenan+APETx2 (b). These examples show a clear increase in spike activity when carrageenan is injected into the tibia in the presence of saline (a), but not when co-administered with APETx2 (b). (c) Frequency histograms of the total number of A $\delta$  fiber spikes isolated from whole-nerve recordings before and after co-application of carrageenan with saline (N = 5) or APETx2 (1  $\mu$ M; N = 6). (d) There was a reduction in the AUC<sub>0-60min</sub> for A $\delta$  fiber spikes in animals treated with APETx2 compared to saline (Unpaired t-test,  $P < 0.001$ ). (e) Frequency histograms of the total number of C fiber spikes isolated from whole-nerve recordings before and after co-application of carrageenan with saline (N = 4) or APETx2 (1  $\mu$ M; N = 5). (f) There was a reduction in the AUC<sub>0-60min</sub> for C fiber spikes in animals treated with APETx2 compared to saline (Unpaired t-test,  $P < 0.001$ ). Bin width = 20 seconds. Data are represented as mean  $\pm$  SEM.

contrast, there was a later (latency to onset of  $9.2 \pm 2.6$  min) and more prolonged carrageenan-induced increase in C fiber activity in these same animals, that lasted for up to 50 minutes (Figure 2(e)). The spike frequency histograms revealed clear decreases in A $\delta$  (Figure 2(c)) and C fiber (Figure 2(e)) activity in animals co-administered with APETx2, relative to those co-administered with saline. There was also a significant decrease in activity, measured as the area under the curve generated from histograms of individual recordings, for both A $\delta$  (Figure 2(d)) and C fiber units (Figure 2(f)). These findings show that inhibition of ASIC3 with APETx2 reduces carrageenan-induced increases in the ongoing activity of A $\delta$  and C bone afferent neurons.

### *Inhibition of ASIC3 attenuates carrageenan-induced sensitization to mechanical stimulation*

To determine if inhibition of ASIC3 could attenuate carrageenan-induced changes in the sensitivity of bone afferent neurons to mechanical stimulation, we compared measures of sensitization to mechanical stimulation in animals administered carrageenan+APETx2, carrageenan+saline or saline alone. There was a clear increase in sensitivity of bone afferent neurons in animals administered carrageenan+saline (Figure 3(b))

relative to those administered saline only (Figure 3(a)), and there was a clear reduction in the sensitivity of bone afferent neurons to the mechanical stimulus in animals administered carrageenan+APETx2 (Figure 3(c)) relative to those administered carrageenan+saline (Figure 3(b)). For analysis of the threshold for activation of single A $\delta$  bone afferent neurons, mixed model analysis with Dunnett's *post hoc* testing (F [7.486], DFn [2], Dfd [18],  $P < 0.05$ ) revealed a reduction in threshold for activation in animals after administration of carrageenan+saline, relative to those administered saline alone (Figure 3(d)), and an increase in the threshold for activation in animals after administration of carrageenan+APETx2, relative to those administered carrageenan+saline (Figure 3(d)). We also classified units as sensitized by carrageenan if their threshold for activation was reduced by more than 20%, relative to the threshold for activation of the same unit before carrageenan was injected, and compared the numbers of sensitized and not-sensitized units in the carrageenan+APETx2 vs carrageenan+saline treated animals. A chi-square test revealed that significantly fewer units were sensitized in animals treated with carrageenan+APETx2 compared to carrageenan+saline (Figure 3(e)). For analysis of the discharge frequency of single A $\delta$  bone afferent neurons, mixed model analysis with Dunnett *post hoc* testing

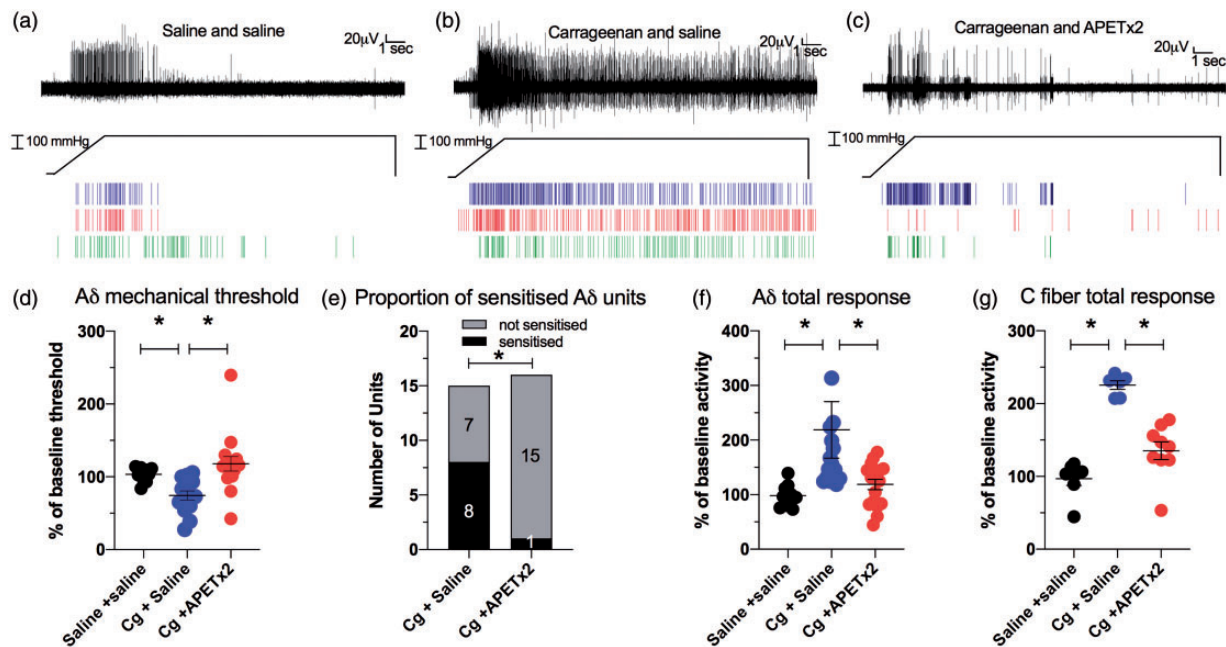


**Figure 3.** Inhibition of ASIC3 with APETx2 inhibits carrageenan-induced mechanical sensitization in A $\delta$  and C fiber bone afferent neurons. (a)–(c) are examples of a whole-nerve recording and rasters of single A $\delta$  fiber neuronal activity in response to a 300 mmHg ramp-and-hold pressure stimulus, in an animal injected with saline only (a), carrageenan+saline (b) and carrageenan+APETx2 (c). These examples show increased spike activity when carrageenan was injected into the tibia with saline (b), relative to when saline was injected into the tibia alone (a), and decreased spike activity when carrageenan was injected into the tibia in the presence of APETx2 (c), relative to when it was injected into the tibia in the presence of saline (b). (d) There was a reduction in threshold for activation of single A $\delta$  fiber units in animals administered carrageenan+saline (N = 7, n = 15), relative to those administered saline alone (N = 7, n = 10) (Dunnett test,  $P < 0.05$ ), and an increase in the threshold for activation in animals administered carrageenan+APETx2 (N = 7, n = 16), relative to those administered carrageenan+saline (Dunnett test,  $P < 0.05$ ). (e) Significantly fewer of the single units were sensitized in animals treated with carrageenan+APETx2 compared to carrageenan+saline (Chi-square test,  $P < 0.05$ ). (f) There was an increase in single A $\delta$  fiber unit discharge frequency in animals administered carrageenan+saline (N = 7, n = 15), relative to those administered saline alone (N = 7, n = 10) (Dunnett test,  $P < 0.05$ ), and a reduction in discharge frequency in animals administered carrageenan+APETx2 (N = 7, n = 16), relative to those administered carrageenan+saline (Dunnett test,  $P < 0.05$ ). (g) There was an increase in C fiber discharge in animals treated with carrageenan+saline (N = 6) relative to animals treated with saline alone (N = 7) (Dunn's test;  $P < 0.05$ ), and reduced C fiber activity for animals treated with carrageenan+APETx2 (N = 9) relative to animals treated with carrageenan+saline (Dunn's test,  $P < 0.05$ ).

(F [7.489], DF<sub>n</sub> [2], Dfd [18],  $P < 0.05$ ) revealed an increase in discharge frequency in animals after administration of carrageenan+saline, relative to those administered saline alone, and a reduction in discharge frequency in animals after administration of carrageenan+APETx2, relative to those administered carrageenan+saline (Figure 3(f)). For analysis of the whole-nerve C fiber discharge frequency, a Kruskal Wallis test with Dunn's *post hoc* testing (KW ANOVA; total response  $H(2) = 16.44$   $P < 0.05$ ) revealed significantly increased C fiber discharge in animals after treatment with carrageenan+saline relative to animals treated with saline alone, and reduced C fiber spike activity for animals after treatment with carrageenan+APETx2 relative to animals treated with carrageenan+saline (Figure 3(g)). Taken together, these findings show that carrageenan sensitizes both A $\delta$  and C fiber bone afferent neurons to mechanical

stimulation, and that APETx2 reduces carrageenan-induced sensitivity of bone afferent neurons to mechanical stimulation.

#### *Inhibition of ASIC3 alone does not affect the ability of bone afferent neurons to respond to mechanical stimulation*

To determine if inhibiting ASIC3 with APETx2 affected the mechanical sensitivity of bone afferent neurons in the absence of inflammation, the threshold for activation and the discharge frequency of bone afferent neurons, in response to mechanical stimulation, was compared in naïve animals treated with APETx2 or saline alone (no carrageenan). There was no difference in the sensitivity of bone afferent neurons to the same mechanical stimulus before (Figure 4(a)) or after APETx2 administration (Figure 4(b)). Comparisons using a nested t-test revealed



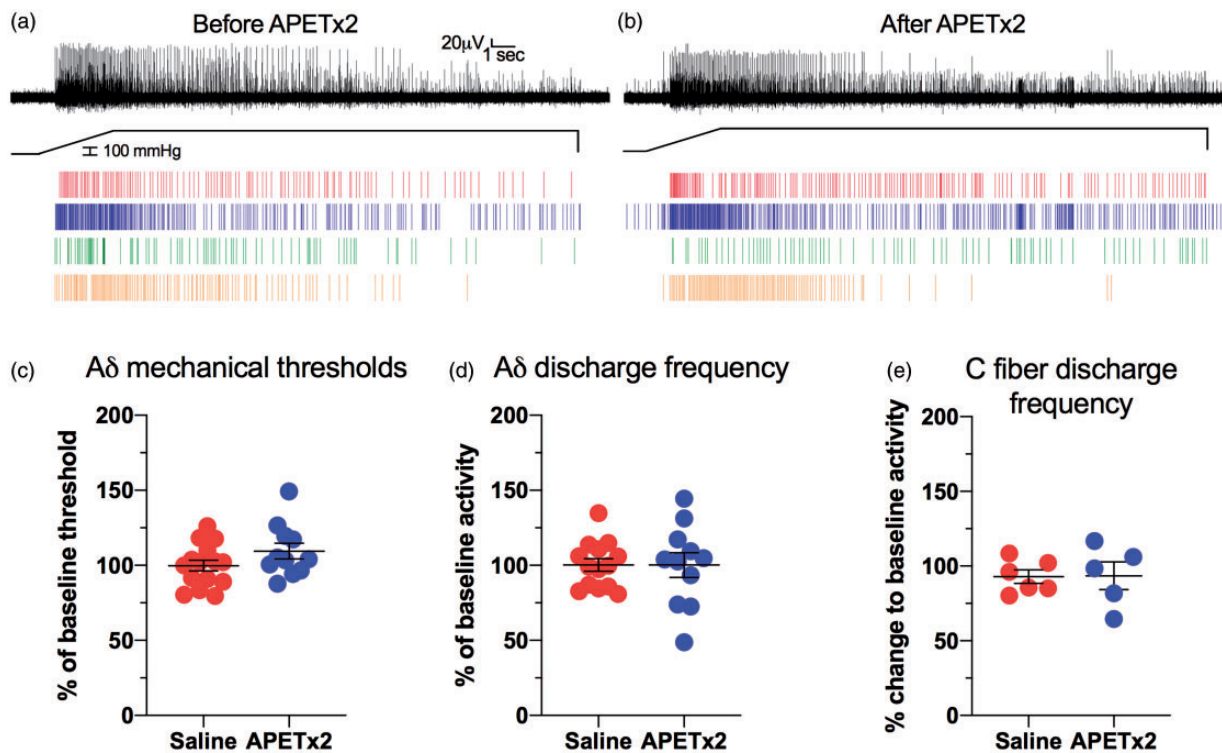


**Figure 4.** Inhibition of ASIC3 with APETx2 does not affect mechanical sensitivity of A $\delta$  and C fiber bone afferent neurons. (a) and (b) are examples of a whole-nerve recording and rasters of single A $\delta$  fiber activity in response to a 300 mmHg ramp-and-hold pressure stimulus, in an animal before (a) and after (b) injection of APETx2. They show no difference in spike activity before (a) or after (b) injection of APETx2. (c) There was no change to threshold for activation of single A $\delta$  fiber units in animals administered APETx2 (N = 5, n = 11), relative to those administered saline alone (N = 7, n = 17) (nested t-test,  $P > 0.05$ ). (d) There was no change to discharge frequency in animals administered APETx2 (N = 5, n = 11), relative to those administered saline alone (N = 7, n = 17) (nested t-test,  $P > 0.05$ ). (f) There was no change to whole-nerve C fiber discharge in animals treated with APETx2 (N = 5), relative to animals treated with saline alone (N = 6) (Mann-Whitney test;  $P > 0.05$ ).

there were no differences between the threshold for activation (Figure 4(c)) or discharge frequency (Figure 4(d)) of A $\delta$  bone afferent neurons in animals injected with saline vs those injected with APETx2. A Mann-Whitney test also revealed no difference in whole-nerve C fiber discharge frequencies in animals after injection of saline vs those injected with APETx2 (Figure 4(e)).

## Discussion

The main findings of the present study are that ASIC3 is expressed in a substantial proportion of bone afferent neurons, and that pharmacological inhibition of ASIC3 with APETx2 reduces carrageenan-induced increases in activity and mechanical sensitivity of A $\delta$  and C fiber bone afferent neurons.

Using retrograde tracing, we found that ASIC3 is expressed in approximately one third of bone afferent neurons, both in unmyelinated (C) and some small diameter myelinated (A $\delta$ ) neurons. This is consistent with our electrophysiological findings showing physiological

effects of ASIC3 inhibition on the activity and sensitivity of both A $\delta$  and C bone afferent neurons after acute inflammation. Our findings are broadly consistent with other studies using retrograde tracers that show ASIC3 expression in 50% of small diameter muscle afferent neurons and 28% of small diameter cutaneous afferent neurons,<sup>42</sup> 43% of thoracolumbar and 42% lumbosacral of colonic sensory afferent neurons,<sup>44</sup> between 18–31% of knee joint afferents,<sup>21</sup> and 33% of trigeminal neurons that project to tooth pulp.<sup>43</sup> We have further shown that the majority of ASIC3 expressing bone afferent neurons co-express CGRP and/or the NGF receptor TrkA, indicating that they are mostly peptidergic, NGF-sensitive nociceptors. NGF-sensitive nociceptors are known to play a central role in regulating inflammatory pain.<sup>45–48</sup> Our finding in the present study of ASIC3 and TrkA co-expression in bone afferent neurons, suggests that NGF-sensitive bone afferent neurons are likely to be important sensors of changes to the pH of the bone microenvironment when inflammation is present.

We have previously shown that activation of TRPV1 (another acid sensing ion channel) sensitizes A $\delta$  and C

fiber bone afferent neurons to mechanical stimulation.<sup>49</sup> Of note, approximately half of the ASIC3 expressing bone afferent neurons we observed in the present study also express TRPV1. There are previous electrophysiological studies demonstrating that many small DRG neurons that have ASIC currents, also possess TRPV1 currents.<sup>50</sup> However, the pH sensitivity of ASIC channels and TRPV1 channels expressed in DRG neurons differ, with proton-gated current activated by  $\text{pH} \geq 6$  being mainly mediated by ASICs in rat DRG neurons.<sup>50</sup> Taken together with our data showing that there may be multiple sub-populations of bone afferent neurons that express TRPV1 and/or ASIC3, these data suggests that there may be heterogeneity in the function of different sub-populations of ASIC3 expressing bone afferent neurons.

Carrageenan is a sulfated polysaccharide that is used to induce acute inflammatory reactions accompanied by hyperalgesia.<sup>51–56</sup> Localized peripheral injections of carrageenan result in rapid infiltration of neutrophils and plasma extravasation of proteins at the site of injection,<sup>55,57,58</sup> and the release from activated immune cells of a number of inflammatory mediators (including histamine, prostaglandins, NGF and bradykinin) and/or endogenous lipid activators (such as arachidonic acid), which are known to interact with peripheral sensory neurons.<sup>46,57,59–65</sup> Our finding that APET×2 reduces carrageenan-induced activity in both A $\delta$  and C bone afferent neurons suggests that ASIC3 modulates, at least in part, acute inflammation-induced activity of bone afferent neurons. Acute pain can be mediated through either direct and/or indirect activation of ASIC3 expressed on the peripheral nerve terminal endings of nociceptors.<sup>16,26,50,66</sup> Direct activation can be via stimulation of ASIC3 embedded in the membrane of nerve terminals by extracellular protons,<sup>67,68</sup> an effect that could be further potentiated by endogenous lipid activators such as arachidonic acid.<sup>65,69</sup> It is unlikely that carrageenan-induced inflammation increases the expression of ASIC3 in bone afferent neurons during our recordings, because there is not enough time for transcriptionally regulated events to occur. However, ASICs are expressed on non-neuronal cell types that reside in bone. Osteoclasts, macrophages and dendritic cells all express ASICs and are themselves able to mediate the effects of acidosis associated with inflammation.<sup>70–73</sup> They can release extracellular protons and cytokines which can indirectly activate ASIC3, or other ion channels and receptors, embedded in the membrane of peripheral nerve terminals.<sup>20</sup> Given that CGRP can cause degranulation of mast cells, and that mast cell mediators increase the proton sensitivity of ASIC3,<sup>74</sup> it is also possible that release of CGRP from peptidergic bone afferent neurons may contribute to mast cell-mediated changes in the sensitivity of ASIC3 expressed

in bone afferent neurons. We cannot differentiate between direct or indirect effects in our preparation.

However, it has been demonstrated that APET×2 directly inhibits C fiber spontaneous nerve activity in response to acidification in a skin-nerve preparation, and injection of moderately acidic solutions under the skin cause spontaneous flinching that is inhibited by co-injection with APET×2.<sup>16</sup> There is also evidence of behavioral effects of ASIC3 inhibition in a model of osteoarthritis, but it is not clear if this was due to effects on neuronal ASIC3, or if it was due to reduced damage to cartilage via actions on ASIC3 expressed by chondrocytes.<sup>21</sup>

Sensitization to mechanical stimulation is a feature that is common to many bony pathologies, including osteoarthritis and bone cancer.<sup>3,75,76</sup> ASICs can be modulated and their currents potentiated by protein kinase C mediated phosphorylation, and nitric oxide dependent s-nitrosylation, augmenting their response to acidification.<sup>77–79</sup> APET×2 acts at the external side of ASIC3 and rapidly inhibits ASIC3 currents induced by acidification.<sup>26</sup> Here we have shown that inhibition of ASIC3 prevents carrageenan-induced sensitization of both A $\delta$  and C bone afferent neurons to mechanical stimulation. This is similar to what is observed for ASIC3 modulation in other tissue types. For example, intra-plantar and intra-muscular carrageenan-induced sensitization is inhibited in ASIC3 KO mice compared to wildtype controls,<sup>80,81</sup> and administration of an acidic inflammatory soup results in the sensitization of muscular and mucosal colonic afferents to mechanical stimulation in control mice, but not in ASIC3 KO mice.<sup>82</sup> While ASIC3 knockout does not abolish mechanically activated currents in cultured DRG neurons,<sup>83</sup> there is some evidence that ASIC3 can act as a mechanoreceptor. A $\delta$  mechanoreceptors recorded in the skin-nerve preparation taken from ASIC3 KO mice have increased sensitivity to mechanical stimulation even in the absence of any inflammation.<sup>66,84</sup> ASIC3 KO mice also display reduced visceral nociception, demonstrated by reductions in colonic afferent activity and impaired visceromotor reflexes in response to a noxious mechanical stimulus.<sup>82,85,86</sup> Knockout of ASIC3 from murine proprioceptors impairs their ability to transduce mechanical stimuli, and the mice have deficits in grid and balance beam walking tasks.<sup>87,88</sup> Our findings show that ASIC3 inhibition with APET×2 has no effect on responses of bone afferent neurons to noxious mechanical stimulation, delivered as increased intraosseous pressure, in naïve animals.

Bisphosphonates are anti-bone resorption drugs which inhibit osteoclast activity prevent acidosis, and relieve pain in patients with osteoporosis<sup>89,90</sup> and in animals with bone cancer.<sup>91,92</sup> This suggests that a large part of the pain phenotype in these bony pathologies may be driven by a change in pH.<sup>93</sup> Blocking ASIC3

with resveratrol or APET $\times$ 2 attenuates pain behaviors in animal models of osteoporosis and bone cancer, further suggesting that modulating ASIC3 function may be of therapeutic benefit in the treatment of pain in these conditions.<sup>20,22</sup> Additionally ASIC3 is upregulated in DRG neurons in animal models of osteoporosis,<sup>6</sup> bone cancer<sup>7,22,23,94</sup> and multiple myeloma.<sup>20</sup> Taken together with the results of the present study, we suggest that ASIC3 expressing bone afferent neurons are activated and/or sensitized by protons and inflammatory mediators to signal pain associated with these conditions. Our findings provide a mechanism to support the therapeutic potential of inhibiting ASIC3 to treat bone pain. Future studies utilizing ASIC3 potentiators, arachidonic acid and lysophosphatidylcholine, in conjunction with acidosis of the bone marrow cavity, may provide further evidence for the contribution of ASIC3 to signaling pain in bony pathology.

### Acknowledgment

The authors acknowledge Associate Professor James Brock for his comments on the manuscript.

### Author Contributions

JJI, MM, JT, PT, MH made substantial contributions to conception and design, or acquisition of data, or analysis and interpretation of data; drafted the article or revised it critically for important intellectual content; and approved the final of the version of the manuscript.






### Declaration of Conflicting Interests

The author(s) declared no potential conflicts of interest with respect to the research, authorship, and/or publication of this article.

### Funding

The author(s) disclosed receipt of the following financial support for the research, authorship, and/or publication of this article: This work was supported by funding from the Australian National Health and Medical Research Council.

### ORCID iDs

Michael Morgan  <https://orcid.org/0000-0002-3641-2774>  
 Jenny Thai  <https://orcid.org/0000-0002-2687-844X>  
 Phu Trinh  <https://orcid.org/0000-0001-9440-2155>  
 Kelly N Effendi  <https://orcid.org/0000-0002-6232-337X>  
 Jason J Ivanusic  <https://orcid.org/0000-0002-7413-5704>

### References

- Berenbaum F. Osteoarthritis as an inflammatory disease (osteoarthritis is not osteoarthrosis!). *Osteoarth Cartil* 2013; 21: 16–21.
- Bove SE, Flatters SJ, Inglis JJ, Mantyh PW. New advances in musculoskeletal pain. *Brain Res Rev* 2009; 60: 187–201.
- Haegerstam GA. Pathophysiology of bone pain: a review. *Acta Orthop Scand* 2001; 72: 308–317.
- Mamet J, Baron A, Lazdunski M, Voilley N. Proinflammatory mediators, stimulators of sensory neuron excitability via the expression of acid-sensing ion channels. *J Neurosci* 2002; 22: 10662–10670.
- Nagae M, Hiraga T, Wakabayashi H, Wang L, Iwata K, Yoneda T. Osteoclasts play a part in pain due to the inflammation adjacent to bone. *Bone* 2006; 39: 1107–1115.
- Kanaya K, Iba K, Abe Y, Dohke T, Okazaki S, Matsumura T, Yamashita T. Acid-sensing ion channel 3 or P2X2/3 is involved in the pain-like behavior under a high bone turnover state in ovariectomized mice. *J Orthop Res* 2016; 34: 566–573.
- Nagae M, Hiraga T, Yoneda T. Acidic microenvironment created by osteoclasts causes bone pain associated with tumor colonization. *J Bone Miner Metab* 2007; 25: 99–104.
- Adami S. Bisphosphonates in prostate carcinoma. *Cancer* 1997; 80: 1674–1679.
- Clohisy DR, Ramnaraine ML. Osteoclasts are required for bone tumors to grow and destroy bone. *J Orthop Res* 1998; 16: 660–666.
- Yoneda T, Hiasa M, Nagata Y, Okui T, White FA. Acidic microenvironment and bone pain in cancer-colonized bone. *Bonekey Rep* 2015; 4: 690.
- Bevan S, Geppetti P. Protons: small stimulants of capsaicin-sensitive sensory nerves. *Trends Neurosci* 1994; 17: 509–512.
- Krishtal OA, Pidoplichko VI. A receptor for protons in the nerve cell membrane. *Neuroscience* 1980; 5: 2325–2327.
- Reeh PW, Steen KH. Tissue acidosis in nociception and pain. *Prog Brain Res* 1996; 113: 143–151.
- Waldmann R. Proton-gated cation channels-neuronal acid sensors in the central and peripheral nervous system. *Adv Exp Med Biol* 2001; 502: 293–304.
- Deval E, Lingueglia E. Acid-Sensing ion channels and nociception in the peripheral and Central nervous systems. *Neuropharmacology* 2015; 94: 49–57.
- Deval E, Noel J, Lay N, Alloui A, Diochot S, Friend V, Jodar M, Lazdunski M, Lingueglia E. ASIC3, a sensor of acidic and primary inflammatory pain. *Embo J* 2008; 27: 3047–3055.
- Fu H, Fang P, Zhou HY, Zhou J, Yu XW, Ni M, Zheng JY, Jin Y, Chen JG, Wang F, Hu ZL. Acid-sensing ion channels in trigeminal ganglion neurons innervating the orofacial region contribute to orofacial inflammatory pain. *Clin Exp Pharmacol Physiol* 2016; 43: 193–202.
- Karczewski J, Spencer RH, Garsky VM, Liang A, Leitl MD, Cato MJ, Cook SP, Kane S, Urban MO. Reversal of acid-induced and inflammatory pain by the selective ASIC3 inhibitor, APET $\times$ 2. *Br J Pharmacol* 2010; 161: 950–960.
- Mogil JS, Breese NM, Witty MF, Ritchie J, Rainville ML, Ase A, Abbadi N, Stucky CL, Seguela P. Transgenic expression of a dominant-negative ASIC3 subunit leads to increased sensitivity to mechanical and inflammatory stimuli. *J Neurosci* 2005; 25: 9893–9901.
- Hiasa M, Okui T, Allette YM, Ripsch MS, Sun-Wada GH, Wakabayashi H, Roodman GD, White FA, Yoneda T. Bone

- pain induced by multiple myeloma is reduced by targeting V-ATPase and ASIC3. *Cancer Res* 2017; 77: 1283–1295.
21. Izumi M, Ikeuchi M, Ji Q, Tani T. Local ASIC3 modulates pain and disease progression in a rat model of osteoarthritis. *J Biomed Sci* 2012; 19: 77.
  22. Zhu H, Ding J, Wu J, Liu T, Liang J, Tang Q, Jiao M. Resveratrol attenuates bone cancer pain through regulating the expression levels of ASIC3 and activating cell autophagy. *Acta Biochim Biophys Sin (Shanghai)* 2017; 49: 1008–1014.
  23. Qiu F, Wei X, Zhang S, Yuan W, Mi W. Increased expression of acid-sensing ion channel 3 within dorsal root ganglia in a rat model of bone cancer pain. *Neuroreport* 2014; 25: 887–893.
  24. Cristofori-Armstrong B, Rash LD. Acid-sensing ion channel (ASIC) structure and function: insights from spider, snake and sea anemone venoms. *Neuropharmacology* 2017; 127: 173–184.
  25. Israel MR, Morgan M, Tay B, Deuis JR. Toxins as tools: fingerprinting neuronal pharmacology. *Neurosci Lett* 2018; 679: 4–14.
  26. Diochot S, Baron A, Rash LD, Deval E, Escoubas P, Scarzello S, Salinas M, Lazdunski M. A new sea anemone peptide, APET×2, inhibits ASIC3, a major acid-sensitive channel in sensory neurons. *Embo J* 2004; 23: 1516–1525.
  27. Diochot S, Salinas M, Baron A, Escoubas P, Lazdunski M. Peptides inhibitors of acid-sensing ion channels. *Toxicon* 2007; 49: 271–284.
  28. Nencini S, Thai J, Ivanusic JJ. Sequestration of artemin reduces inflammation-induced activation and sensitization of bone marrow nociceptors in a rodent model of Carrageenan-induced inflammatory bone pain. *Eur J Pain* 2019; 23: 397–409.
  29. Nencini S, Ringuet M, Kim DH, Greenhill C, Ivanusic JJ. GDNF, neurturin, and artemin activate and sensitize bone afferent neurons and contribute to inflammatory bone pain. *J Neurosci* 2018; 38: 4899–4911.
  30. Nencini S, Ringuet M, Kim DH, Chen YJ, Greenhill C, Ivanusic JJ. Mechanisms of nerve growth factor signaling in bone nociceptors and in an animal model of inflammatory bone pain. *Mol Pain* 2017; 13: 174480691769701.
  31. Nencini S, Ivanusic J. Mechanically sensitive adelta nociceptors that innervate bone marrow respond to changes in intra-osseous pressure. *J Physiol* 2017; 595: 4399–4415.
  32. Blanchard MG, Rash LD, Kellenberger S. Inhibition of voltage-gated Na(+) currents in sensory neurones by the sea anemone toxin APET×2. *Br J Pharmacol* 2012; 165: 2167–2177.
  33. Jensen JE, Durek T, Alewood PF, Adams DJ, King GF, Rash LD. Chemical synthesis and folding of APET×2, a potent and selective inhibitor of acid sensing ion channel 3. *Toxicon* 2009; 54: 56–61.
  34. Yen LD, Bennett GJ, Ribeiro-da-Silva A. Sympathetic sprouting and changes in nociceptive sensory innervation in the glabrous skin of the rat hind paw following partial peripheral nerve injury. *J Comp Neurol* 2006; 495: 679–690.
  35. Lorenzo LE, Ramien M, St Louis M, De Koninck Y, Ribeiro-da-Silva A. Postnatal changes in the rexed lamination and markers of nociceptive afferents in the superficial dorsal horn of the rat. *J Comp Neurol* 2008; 508: 592–604.
  36. Fukuoka T, Kobayashi K, Yamanaka H, Obata K, Dai Y, Noguchi K. Comparative study of the distribution of the alpha-subunits of voltage-gated sodium channels in normal and axotomized rat dorsal root ganglion neurons. *J Comp Neurol* 2008; 510: 188–206.
  37. Han HM, Kim TH, Bae JY, Bae YC. Primary sensory neurons expressing tropomyosin receptor kinase a in the rat trigeminal ganglion. *Neurosci Lett* 2019; 690: 56–60.
  38. Everaerts W, Sepulveda MR, Gevaert T, Roskams T, Nilius B, De Ridder D. Where is TRPV1 expressed in the bladder, do we see the real channel? *Naunyn Schmiedebergs Arch Pharmacol* 2009; 379: 421–425.
  39. Alamri A, Bron R, Brock JA, Ivanusic JJ. Transient receptor potential cation channel subfamily V member 1 expressing corneal sensory neurons can be subdivided into at least three subpopulations. *Front Neuroanat* 2015; 9: 71.
  40. Ivanusic JJ. Size, Neurochemistry, and Segmental Distribution of Sensory Neurons Innervating the Rat Tibia. *J Comp Neurol* 2009; 517: 276–283.
  41. Lee CH, Sun SH, Lin SH, Chen CC. Role of the acid-sensing ion channel 3 in blood volume control. *Circ J* 2011; 75: 874–883.
  42. Molliver DC, Immke DC, Fierro L, Pare M, Rice FL, McCleskey EW. ASIC3, an acid-sensing ion channel, is expressed in metaboreceptive sensory neurons. *Mol Pain* 2005; 1: 1744–8069.
  43. Ichikawa H, Sugimoto T. The co-expression of ASIC3 with calcitonin gene-related peptide and parvalbumin in the rat trigeminal ganglion. *Brain Res* 2002; 943: 287–291.
  44. Christianson JA, Traub RJ, Davis BM. Differences in spinal distribution and neurochemical phenotype of colonic afferents in mouse and rat. *J Comp Neurol* 2006; 494: 246–259.
  45. Jankowski MP, Koerber HR. Neurotrophic factors and nociceptor sensitization. In: Kruger L and Light AR (eds) *Translational pain research: from mouse to man*. Boca Raton: CRC Press, 2010; 43: 31–50.
  46. Koltzenburg M, Bennett DL, Shelton DL, McMahon SB. Neutralization of endogenous NGF prevents the sensitization of nociceptors supplying inflamed skin. *Eur J Neurosci* 1999; 11: 1698–1704.
  47. McMahon SB. NGF as a mediator of inflammatory pain. *Philos Trans R Soc Lond B Biol Sci* 1996; 351: 431–440.
  48. Weskamp G, Otten U. An enzyme-linked immunoassay for nerve growth factor (NGF): a tool for studying regulatory mechanisms involved in NGF production in brain and in peripheral tissues. *J Neurochem* 1987; 48: 1779–1786.
  49. Morgan M, Nencini S, Thai J, Ivanusic JJ. TRPV1 activation alters the function of adelta and C fiber sensory neurons that innervate bone. *Bone* 2019; 123: 168–175.
  50. Poirot O, Berta T, Decosterd I, Kellenberger S. Distinct ASIC currents are expressed in rat putative nociceptors and are modulated by nerve injury. *J Physiol* 2006; 576: 215–234.

51. Sugishita E, Amagaya S, Ogihara Y. Anti-inflammatory testing methods: comparative evaluation of mice and rats. *J Pharmacobiodyn* 1981; 4: 565–575.
52. Henriques MG, Silva PM, Martins MA, Flores CA, Cunha FQ, Assreuy-Filho J, Cordeiro RS. Mouse paw edema: a new model for inflammation? *Braz J Med Biol Res* 1987; 20: 243–249.
53. Jain NK, Patil CS, Singh A, Kulkarni SK. Sildenafil-induced peripheral analgesia and activation of the nitric oxide-cyclic GMP pathway. *Brain Res* 2001; 909: 170–178.
54. Petersson M, Wiberg U, Lundeborg T, Uvnas-Moberg K. Oxytocin decreases carrageenan induced inflammation in rats. *Peptides* 2001; 22: 1479–1484.
55. Posadas I, Bucci M, Roviezzo F, Rossi A, Parente L, Sautebin L, Cirino G. Carrageenan-induced mouse paw oedema is biphasic, age-weight dependent and displays differential nitric oxide cyclooxygenase-2 expression. *Br J Pharmacol* 2004; 142: 331–338.
56. Radhakrishnan R, Moore SA, Sluka KA. Unilateral carrageenan injection into muscle or joint induces chronic bilateral hyperalgesia in rats. *Pain* 2003; 104: 567–577.
57. Capasso F, Dunn CJ, Yamamoto S, Willoughby DA, Giroud JP. Further studies on carrageenan-induced pleurisy in rats. *J Pathol* 1975; 116: 117–124.
58. Vinegar R, Truax JF, Selph JL. Quantitative studies of the pathway to acute carrageenan inflammation. *Fed Proc* 1976; 35: 2447–2456.
59. Tsuchida K, Ibuki T, Matsumura K. Bromoenol lactone, an inhibitor of calcium-independent phospholipase A2, suppresses Carrageenan-induced prostaglandin production and hyperalgesia in rat hind paw. *Mediators Inflamm* 2015; 2015: 605727.
60. Valenti C, Giuliani S, Cialdai C, Tramontana M, Maggi CA. Anti-inflammatory synergy of MEN16132, a kinin B (2) receptor antagonist, and dexamethasone in carrageenan-induced knee joint arthritis in rats. *Br J Pharmacol* 2010; 161: 1616–1627.
61. Fernandez-Duenas V, Sanchez S, Planas E, Poveda R. Adjuvant effect of caffeine on acetylsalicylic acid antinociception: prostaglandin E2 synthesis determination in carrageenan-induced peripheral inflammation in rat. *Eur J Pain* 2008; 12: 157–163.
62. Al-Haboubi HA, Zeitlin IJ. Re-appraisal of the role of histamine in carrageenan-induced paw oedema. *Eur J Pharmacol* 1983; 88: 169–176.
63. Di Rosa M, Giroud JP, Willoughby DA. Studies on the mediators of the acute inflammatory response induced in rats in different sites by carrageenan and turpentine. *J Pathol* 1971; 104: 15–29.
64. Costello AH, Hargreaves KM. Suppression of carrageenan-induced hyperalgesia, hyperthermia and edema by a Bradykinin antagonist. *Eur J Pharmacol* 1989; 171: 259–263.
65. Marra S, Ferru-Clement R, Breuil V, Delaunay A, Christin M, Friend V, Sebille S, Cognard C, Ferreira T, Roux C, Euller-Ziegler L, Noel J, Lingueglia E, Deval E. Non-acidic activation of pain-related acid-sensing ion channel 3 by lipids. *Embo J* 2016; 35: 414–428.
66. Price MP, McIlwrath SL, Xie J, Cheng C, Qiao J, Tarr DE, Sluka KA, Brennan TJ, Lewin GR, Welsh MJ. The DRASIC cation channel contributes to the detection of cutaneous touch and acid stimuli in mice. *Neuron* 2001; 32: 1071–1083.
67. Waldmann R, Champigny G, Bassilana F, Heurteaux C, Lazdunski M. A proton-gated cation channel involved in acid-sensing. *Nature* 1997; 386: 173–177.
68. Olson TH, Riedl MS, Vulchanova L, Ortiz-Gonzalez XR, Elde R. An acid sensing ion channel (ASIC) localizes to small primary afferent neurons in rats. *Neuroreport* 1998; 9: 1109–1113.
69. Lo TN, Saul WF, Lau SS. Carrageenan-stimulated release of arachidonic acid and of lactate dehydrogenase from rat pleural cells. *Biochem Pharmacol* 1987; 36: 2405–2413.
70. Li WG, Xu TL. ASIC3 channels in multimodal sensory perception. *ACS Chem Neurosci* 2011; 2: 26–37.
71. Tong J, Wu WN, Kong X, Wu PF, Tian L, Du W, Fang M, Zheng F, Chen JG, Tan Z, Gong F. Acid-sensing ion channels contribute to the effect of acidosis on the function of dendritic cells. *J Immunol* 2011; 186: 3686–3692.
72. Kong X, Tang X, Du W, Tong J, Yan Y, Zheng F, Fang M, Gong F, Tan Z. Extracellular acidosis modulates the endocytosis and maturation of macrophages. *Cell Immunol* 2013; 281: 44–50.
73. Gregory NS, Brito RG, Fusaro M, Sluka KA. ASIC3 is required for development of fatigue-induced hyperalgesia. *Mol Neurobiol* 2016; 53: 1020–1030.
74. Yan J, Wei X, Bischoff C, Edelmayer RM, Dussor G. pH-evoked dural afferent signaling is mediated by ASIC3 and is sensitized by mast cell mediators. *Headache* 2013; 53: 1250–1261.
75. Honore P, Mantyh PW. Bone cancer pain: from mechanism to model to therapy. *Pain Med* 2000; 1: 303–309.
76. Portenoy RK, Payne D, Jacobsen P. Breakthrough pain: characteristics and impact in patients with cancer pain. *Pain* 1999; 81: 129–134.
77. Cadiou H, Studer M, Jones NG, Smith ES, Ballard A, McMahon SB, McNaughton PA. Modulation of acid-sensing ion channel activity by nitric oxide. *J Neurosci* 2007; 27: 13251–13260.
78. Deval E, Salinas M, Baron A, Lingueglia E, Lazdunski M. ASIC2b-dependent regulation of ASIC3, an essential acid-sensing ion channel subunit in sensory neurons via the partner protein PICK-1. *J Biol Chem* 2004; 279: 19531–19539.
79. Wu J, Liu TT, Zhou YM, Qiu CY, Ren P, Jiao M, Hu WP. Sensitization of ASIC3 by proteinase-activated receptor 2 signaling contributes to acidosis-induced nociception. *J Neuroinflammation* 2017; 14: 150.
80. Sluka KA, Radhakrishnan R, Benson CJ, Eshcol JO, Price MP, Babinski K, Audette KM, Yeomans DC, Wilson SP. ASIC3 in muscle mediates mechanical, but not heat, hyperalgesia associated with muscle inflammation. *Pain* 2007; 129: 102–112.
81. Yen YT, Tu PH, Chen CJ, Lin YW, Hsieh ST, Chen CC. Role of acid-sensing ion channel 3 in sub-acute-phase inflammation. *Mol Pain* 2009; 5: 1.

82. Jones RC, Xu L, Gebhart GF. The mechanosensitivity of mouse colon afferent fibers and their sensitization by inflammatory mediators require transient receptor potential vanilloid 1 and acid-sensing ion channel 3. *J Neurosci* 2005; 25: 10981–10989.
83. Drew LJ, Rohrer DK, Price MP, Blaver KE, Cockayne DA, Cesare P, Wood JN. Acid-sensing ion channels ASIC2 and ASIC3 do not contribute to mechanically activated currents in mammalian sensory neurones. *J Physiol* 2004; 556: 691–710.
84. Chen CC, Zimmer A, Sun WH, Hall J, Brownstein MJ, Zimmer A. A role for ASIC3 in the modulation of high-intensity pain stimuli. *Proc Natl Acad Sci U S A* 2002; 99: 8992–8997.
85. Page AJ, Brierley SM, Martin CM, Hughes PA, Blackshaw LA. Acid sensing ion channels 2 and 3 are required for inhibition of visceral nociceptors by benzamil. *Pain* 2007; 133: 150–160.
86. Page AJ, Brierley SM, Martin CM, Price MP, Symonds E, Butler R, Wemmie JA, Blackshaw LA. Different contributions of ASIC channels 1a, 2, and 3 in gastrointestinal mechanosensory function. *Gut* 2005; 54: 1408–1415.
87. Cheng YR, Jiang BY, Chen CC. Acid-sensing ion channels: dual function proteins for chemo-sensing and mechano-sensing. *J Biomed Sci* 2018; 25: 46.
88. Lin SH, Cheng YR, Banks RW, Min MY, Bewick GS, Chen CC. Evidence for the involvement of ASIC3 in sensory mechanotransduction in proprioceptors. *Nat Commun* 2016; 7: 11460.
89. Iwamoto J, Takeda T, Sato Y, Uzawa M. Effects of alendronate on metacarpal and lumbar bone mineral density, bone resorption, and chronic back pain in postmenopausal women with osteoporosis. *Clin Rheumatol* 2004; 23: 383–389.
90. Ohtori S, Akazawa T, Murata Y, Kinoshita T, Yamashita M, Nakagawa K, Inoue G, Nakamura J, Orita S, Ochiai N, Kishida S, Takaso M, Eguchi Y, Yamauchi K, Suzuki M, Aoki Y, Takahashi K. Risedronate decreases bone resorption and improves low back pain in postmenopausal osteoporosis patients without vertebral fractures. *J Clin Neurosci* 2010; 17: 209–213.
91. Jimenez Andrade JM, Mantyh P. Cancer pain: from the development of mouse models to human clinical trials. In: Kruger L, Light AR (eds) *Translational pain research: from mouse to man* (pp. 77–98). Boca Raton: CRC Press, 2010.
92. Sevcik MA, Luger NM, Mach DB, Sabino MA, Peters CM, Ghilardi JR, Schwei MJ, Rohrich H, De Felipe C, Kuskowski MA, Mantyh PW. Bone cancer pain: the effects of the bisphosphonate alendronate on pain, skeletal remodeling, tumor growth and tumor necrosis. *Pain* 2004; 111: 169–180.
93. Di Pompo G, Lemma S, Canti L, Rucci N, Ponzetti M, Errani C, Donati DM, Russell S, Gillies R, Chano T, Baldini N, Avnet S. Intratumoral acidosis fosters cancer-induced bone pain through the activation of the mesenchymal tumor-associated stroma in bone metastasis from breast carcinoma. *Oncotarget* 2017; 8: 54478–54496.
94. Yoneda T, Hata K, Nakanishi M, Nagae M, Nagayama T, Wakabayashi H, Nishisho T, Sakurai T, Hiraga T. Involvement of acidic microenvironment in the pathophysiology of cancer-associated bone pain. *Bone* 2011; 48: 100–105.